Available online at www.sciencedirect.com
ScienceDirect
Trans. Nonferrous Met. Soc. China 21(2011) 278−286
Transactions of Nonferrous Metals Society of China
www.tnmsc.cn

Effect of pulsed current on temperature distribution, weld bead profiles and characteristics of gas tungsten arc welded aluminum alloy joints

N. KARUNAKARAN[1], V. BALASUBRAMANIAN[2]

1. Department of Mechanical Engineering, Annamalai University, Annamalai Nagar 608002, India;
2. Centre for Materials Joining and Research, Department of Manufacturing Engineering, Annamalai University, Annamalai Nagar 608002, India

Received 23 February 2010; accepted 23 April 2010

Abstract: Temperature distribution and weld bead profiles of constant current and pulsed current gas tungsten arc welded aluminium alloy joints were compared. The effects of pulsed current welding on tensile properties, hardness profiles, microstructural features and residual stress distribution of aluminium alloy joints were reported. The use of pulsed current technique is found to improve the tensile properties of the weld compared with continuous current welding due to grain refinement occurring in the fusion zone.
Key words: aluminium alloy; gas tungsten arc welding; pulsed current; temperature distribution; bead profiles; tensile properties

1 Introduction

Reduction of mass is a prime concern for many industries involved in transportation especially the automobile industry, which has become significant because of fuel saving, reduction of emission and recyclability. Hence the focus on light weight materials like aluminium and magnesium has become predominant. Weldability of aluminium alloys has recently been investigated through a variety of processes, such as gas tungsten arc welding (GTAW), gas metal arc welding (GMAW) and friction stir welding[1−2].

In conventional welding, fusion zones typically exhibit coarse columnar grains because of the prevailing thermal conditions during weld metal solidification. This often results in inferior weld mechanical properties and poor resistance to hot cracking. It is thus highly desirable to control solidification structure in welds, but the control is often very difficult because of higher temperatures and higher thermal gradients in welds in relation to castings and the epitaxial nature of the growth process. Nevertheless, several methods for refining weld fusion zones have been tried with some success in the past: inoculation with heterogeneous nucleants, microcooler additions, surface nucleation induced by gas impingement and introduction of physical disturbance through techniques such as torch vibration[3]. In this process, two relatively new techniques, namely, magnetic arc oscillation and current pulsing, have gained wide popularity because of their striking promise and the relative ease and can be applied to actual industrial situations with only minor modifications of the existing welding equipment[4].

Pulsed current GTA welding, developed in 1950s, is a variation of GTA welding which involves cycling of the welding current from a high level to a low level at a selected regular frequency. The high level of the peak current is generally selected to give adequate penetration and bead contour, while the low level of the background current is set at a level sufficient to maintain a stable arc. This permits arc energy to be used efficiently to fuse a spot of controlled dimensions in a short time producing the weld as a series of overlapping nuggets, and limits the wastage of heat by conduction into the adjacent parent material in normal constant current welding. In contrast to constant current welding, the fact that heat energy required to melt the base material is supplied only during peak current pulses for brief intervals of time allows the heat to dissipate into the base material, leading to a narrower heat affected zone (HAZ). The technique has secured a niche for itself in specific applications such

Corresponding author: N. KARUNAKARAN; E-mail: cdl.karun28@gmail.com
DOI: 10.1016/S1003-6326(11)60710-3

as in welding of root passes of tubes, and in welding thin sheets, where precise control over penetration and heat input are required to avoid burn through[5].

Extensive research has been performed on this process and reported advantages include improved bead contour, greater tolerance to heat sink variations, lower heat input requirements, reduced residual stresses and distortion[6]. Metallurgical advantages of pulsed current welding frequently reported in literature include refinement of fusion zone grain size and substructure, reduced width of HAZ, control of segregation, etc[7]. All these factors will help to improve mechanical properties. Current pulsing has been used by several investigators to obtain grain refinement in weld fusion zones and improvement in weld mechanical properties[8−9]. However, reported research work on the effect of pulsed current on temperature distribution and bead profiles and their subsequent influence on tensile properties, hardness profiles and microstructure characteristics are very scant. Hence, the present study was carried out to understand the effect of pulsed current welding technique on the peak temperature, the cooling rate, the cross sectional weld bead profile, the microhardness, the residual stress distribution, the microstructure and the tensile properties of gas tungsten arc welded AA6351-T6 aluminium alloy joints.

2 Experimental procedure

In this investigation, plates with 4 mm in thickness were used as the base materials. The chemical compositions and mechanical properties of base metal are presented in Tables 1 and 2. These plates of aluminium alloy were cut to the required size (150 mm × 150 mm) by power hacksaw cutting and grinding. Square butt joint configuration was used to fabricate the welded joints. Single pass, autogenous welding procedure (without filler metal addition) was applied to fabricating the joints. High purity (99.99%) argon gas was used as shielding gas with a flow rate of 9 L/min. 2% thoriated tungsten electrode with 3.2 mm in diameter was used with DC straight polarity (electrode "−" and base plate "+") to carry out the experiments. The power source used in this investigation is capable of delivering pulsed current in DC mode only. The arc length was maintained at 2 mm.

Table 1 Chemical compositions of base metal (mass fraction, %)

Mg	Si	Fe	Cu
0.7	1.2	0.5	0.1
Mn	Zn	Zr	Al
0.6	0.2	0.05	Bal.

Table 2 Mechanical properties of base metal

Yield strength/ MPa	Tensile strength/ MPa	Elongation in 50 mm length /%	Micro hardness at 0.49 N load (HV)
150	250	20	95

The experimental setup is shown in Fig.1. The welding parameters were controlled by the Lincoln Electric TIG welding machine (Precision TIG 375). To measure the temperature during welding, the K type chromel-alumel thermocouple was used[10−12]. The hot end diameter of the thermocouple was 1.5 mm, the cold end was fixed to a thermocouple bank and was in turn connected to the DAQ Labview. Labview was a bundled package on virtual instrumentation having the flexibility to measure the parameter of concern at very short interval. Fig.2 shows the positions on the plate where the thermocouples were glued to a depth of 2 mm, the holes were drilled at the bottom of the plate[13]. The data acquisition system of LABVIEW was used to acquire the temperature during weld from these three locations as well as the room temperature.

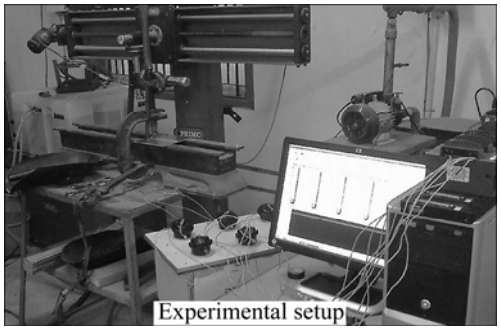

Fig.1 Experimental setup

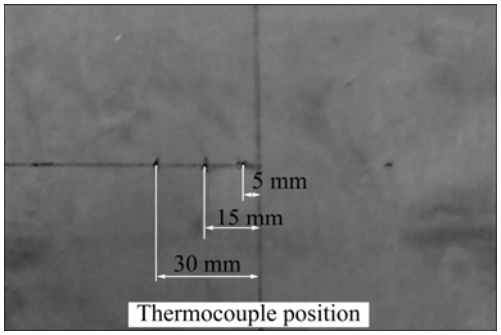

Fig.2 Thermocouple positions on plate

Before welding was performed, the plate was cleaned and thermocouples were incorporated at its appropriate positions. Welding was done by both the constant current (CC) and the pulsed current (PC) process. A number of trial runs on the base material were done to fix the upper and lower heat input levels. The CC higher than 120 A resulted in burning of base metal and in PC process the burning happened above 160 A.

LU and KOU[10] reported that for the GTA welding process, the molten surface is turbulent if the welding current is more than 225 A. The frequency was fixed at 6 Hz[14]. The welding parameters used in this work are listed in Tables 3 and 4. For the calculation of the heat input (Q), the relationship used for constant current process was $Q=(VxI/s)\eta$, where V is the voltage, I is the current, s is the welding speed and η is the efficiency of utilization of the heat generated[15−16]. The calculation of heat input for the pulsed current process was done by computing the mean current using the relationship $I_m=(I_p t+I_b t_b)/ t_T$, where I_m is the mean current, I_p is the peak current, I_b is the base current, t_p is the time on peak pulse, t_b is the time on base current and t_T is the total time[16−18]. From this, the RMS value of current or the effective current was computed and the heat input values are listed in Table 4. Both the processes were performed at the same welding speed and the efficiency of utilization of the heat generated was taken as 70%[15−16].

3 Results

3.1 Temperature profiles

The temperatures at 5, 15 and 30 mm from the weld bead centre were measured for 250 s. The DAQ Labview was used to obtain the temperatures at an interval of 1 s[12]. The heating and cooling curves for the various heat input levels are shown in Table 5. The values of peak temperature are presented in Table 6. The heat input of 312 J/mm for constant current resuted in cracks in the weld, hence the values of temperature profile were not recorded. The cooling rate was determined for the temerature drop from 400 to 200 °C[19]. The values for the location of 5 mm from weld centre with the peak temperature are shown in Table 6.

3.2 Bead profiles

The weld pool shape, cooling rates, weld metal composition and grain growth rates are all interrelated to the heat input in the base metal during welding. The rate of heat input during welding and the cooling rate after welding strongly influence the grain size and phase formation. Hence, it is imperative to understand the effect of various levels of heat input and its influence on the bead profile. Specimens were extracted from the mid portion of the welded plates. The cross sectional surface was polished using standard metallographic procedures and etched with Kellers aqua-reagent to get the clear bead profile. The bead profiles were taken using sterozoom microscope. The weld bead profiles and related dimensions are presented in Table 5.

4 Characteristics of welded joints

The various penetration that was achieved during welding was compared. The joint fabricated at 120 A in constant current had a penetration of 1.45 mm, while the joint welded at 140 A of pulsed current had penetration of 1.52 mm. The ratios of penetration to plate thickness were 0.36 for constant current and 0.38 for pulsed current. These two joints exhibited similar physical characteristics The other characteristics of the joints

Table 3 Constant current welding parameters

Experiment No.	Current/A	Voltage/V	Welding speed/(mm·s^{-1})	Efficiency/%	Heat input/(J·mm^{-1})
1	110	12.5	4.167	70	231
2	120	12.7	4.167	70	256
3	130	12.2	4.167	70	266
4	140	12.5	4.167	70	294
5	150	12.4	4.167	70	312

Table 4 Pulsed current welding parameters

Experiment No.	Peak current/ A	Base current/ A	Voltage/ V	Pulse on time/ %	Frequency/ Hz	Welding speed/ (mm·s^{-1})	Efficiency/ %	Heat input/ (J·mm^{-1})
1	110	55	11	50	6	4.167	70	161
2	120	60	12	50	6	4.167	70	191
3	130	65	13	50	6	4.167	70	224
4	140	70	12.5	50	6	4.167	70	232
5	150	75	13.5	50	6	4.167	70	269

Table 5 Cross sectional profile of weld beads

Current/A	Cross sectional profile		*P/T		W/P*	
	CC	PC	CC	PC	CC	PC
110	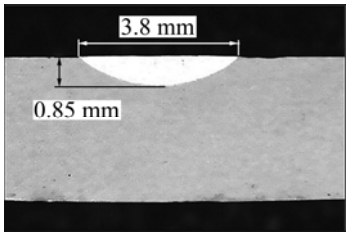	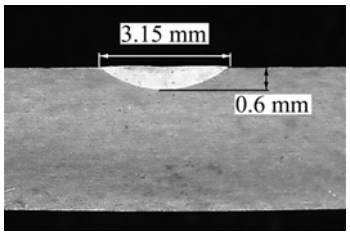	0.22	0.15	5.50	5.25
120	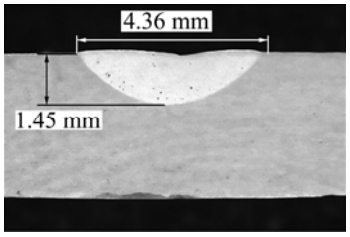	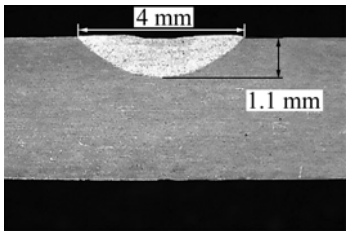	0.36	0.28	3.00	3.64
130	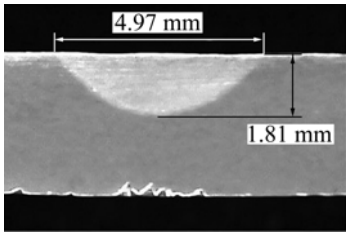	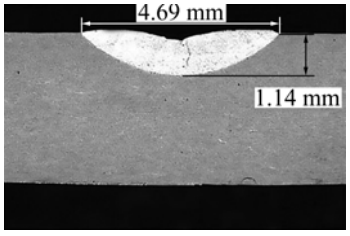	0.45	0.29	2.75	4.11
140	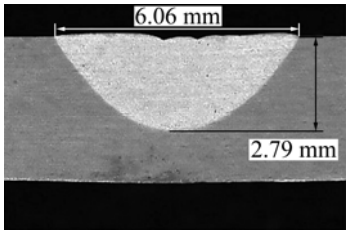	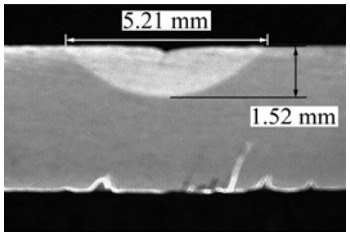	0.70	0.38	2.17	3.43
150	Profile not available	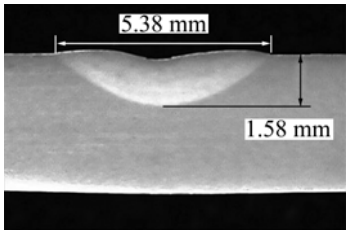	−	0.40	−	3.41

*P: Depth of penetration; W: Width of weld bead; T: Plate thickness

Table 6 Peak temperature values

Experiment No.	Current/A	Heat input/(J·mm^{-1})		Peak temperature at 5 mm/K		Cooling rate/(°C·s^{-1})		Peak temperature at 15 mm/K	
		CC	PC	CC	PC	CC	PC	CC	PC
1	110	231	161	586	589	16.1	19.2	475	460
2	120	256	191	648	609	14.4	13.5	510	477
3	130	266	224	666	626	12.7	13.0	519	484
4	140	294	232	710	704	11.8	12.9	544	505
5	150	312	269	−	707	−	11.9	−	516

like the tensile properties, microhardness, microstructure and the residual stress were compared for these two joints.

4.1 Tensile properties

The transverse tensile properties of the welded joints were evaluated using the universal testing machine (UTM). The 4 mm-thick welded plates were machined (ground) to 1.5 mm-thin sheets in order to have full penetration joints. The specimens were prepared as per the ASTM E8-04 standards and three specimens for each joint were tested and the values are presented in Table 7.

Table 7 Tensile properties of welded joints

Process	Yield strength/ MPa	Tensile strength/ MPa	Elongation/ %	Joint efficiency/ %
Constant current	185	200	8	80
Pulsed current	205	225	10	90

4.2 Hardness

A microhardness testing machine (SHIMADZU HMV−2 Version 2.02) was used to measure the hardness at the weld bead, 5 mm and 15 mm from the weld centre. A load of 0.49 N was applied for 15 s to obtain the Vickers hardness $HV_{0.05}$. Table 8 lists the Vickers hardness values for the two joints at weld zone, 5 mm and 15mm from weld bead centre for constant current and pulsed current.

Table 8 Microhardness (HV) profile

Process	Microhardness (HV)			
	Weld centre	5 mm from weld centre	15 mm from weld centre	Base metal
Constant current	72	84	92	95
Pulsed current	81	88	93	95

4.3 Microstructure

The strength of the weld metal is characterized by the grain size and the phases present in the microstructure. The phase formation and grain growth are highly influenced by the thermal cycle of the welding process. The interesting region of would be the weld metal and the interface zones because at the weld metal the temperature goes to the peak and cools rapidly thus formation of finer grain sizes. The welded specimen was prepared using the standard metallographic procedure, and the polished surfaces were etched with aqua-reagent to get the clear microscopic view of the weldment. The optical microscope (MEIJI Japan Model MIL7100) was used with the software Metalvision MVLx 1.0. The results of the microstructure at the interface region, the weld centre and the heat affected zone (HAZ) are presented in Fig.3.

4.4 Residual stress

The residual stress distribution in the transverse direction was measured by the X-ray diffraction method. The equipment used to mesasure the stress was X3000 (Ver 1.22.9). The software stress tech was used to compile the value of stress from the measured value of "*d* " in the Bragg's equation. The residual stress was measured at the weld bead, 5 mm and 10mm from the weld bead centre. The values of the residual stress are presented in Table 9.

Table 9 Residual stress distribution

Process	Residul stress/MPa			
	Weld centre	5 mm from weld centre	15 mm from weld centre	Base metal
Constant current	134	92	−60.5	−38.4
Pulsed current	112	74	−55.6	−36.3

5 Discussion

5.1 Effect of pulse current on temperature profile

The total time of welding was 36 s. It was seen that when the torch was nearing the line of thermocouple, the maximum temperatures were obtained in all the cases. The peak temperature increases as the heat input increases in all the cases. In constant current process, the highest temperature was 710 K for the higher heat input of 294 J/mm and the lowest was 586 K for 231 J/mm at the 5 mm-distance (Fig.4(a)). In the pulsed current process, for the 5 mm-distance the highest temperature was 707 K for the heat input of 269 J/mm and the lowest peak temperature of 589 K for a heat input of 161 J/mm (Fig.4(c)).

From the temperature profiles, closer to the weld bead (5 mm), it was seen that under constant current conditions, when the heat input was 256 J/mm, metals tended to cluster together above the peak temperatures of about 675 K. The heat input less than 256 J/mm saw a lower peak temperature of less than 585 K. The reason for this can be attributed to the temperature dependent properties of aluminium alloy. This was not predominant in the pulsed current process, and the profile showed uniform temperature variation, which can be attributed to the pulsing of the current.

The profiles of temperature at 15 mm from the centre of the weld bead in constant current and pulsed current processes followed a similar pattern, but the pulsed current showed more uniform cooling pattern, while for lower heat inputs the clustering could be noticed in pulsed current process. When the peak

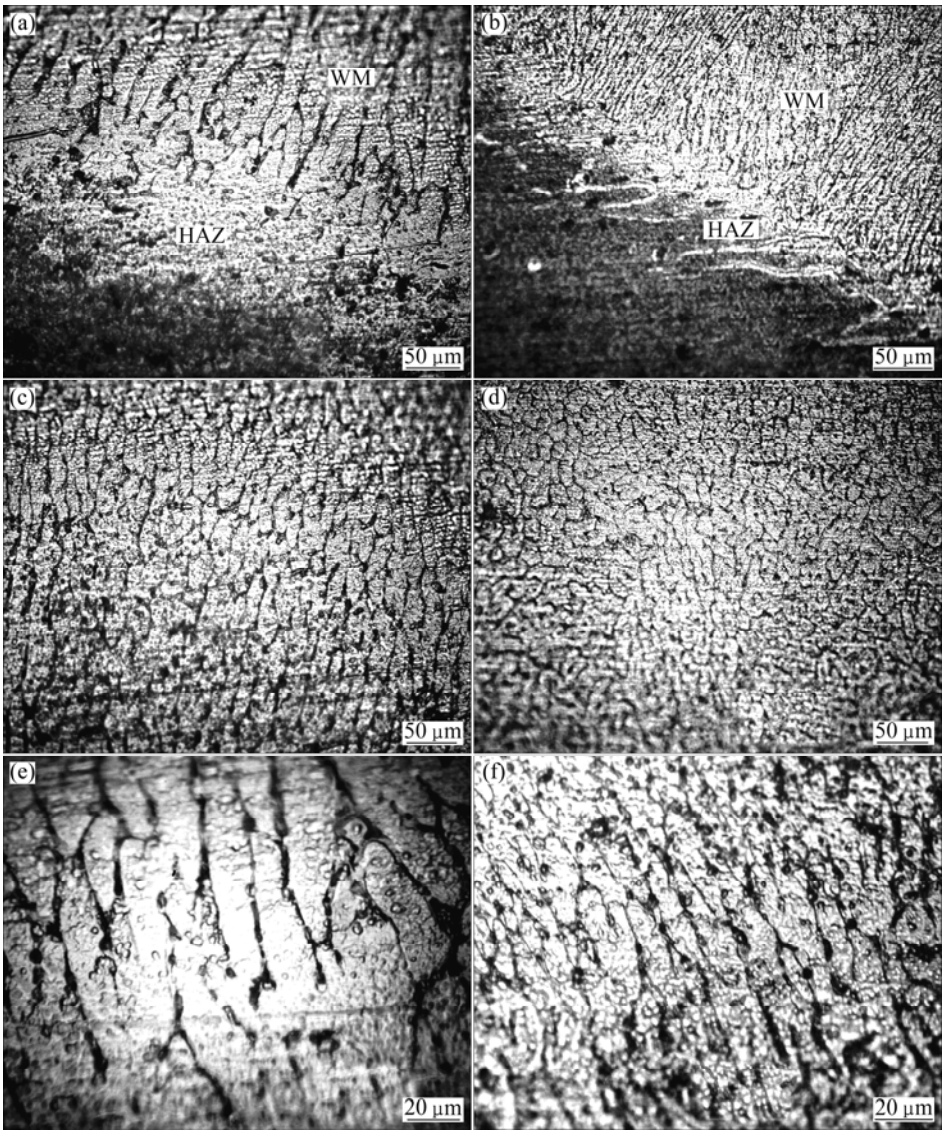

Fig.3 Optical micrographs: (a) Weld metal/HAZ interface (CC); (b) Weld metal/HAZ interface (PC); (c) Weld metal (CC); (d) Weld metal (PC); (e) HAZ (CC); (f) HAZ (PC)

temperature was lower than 500 K, the clustering is seen. This clustering can be attributed to the various thermal properties of aluminium alloy.

The cooling rate presented in Table 6 shows that for the lower heat input rates the cooling rate is slower, but for higher heat inputs the cooling rate is faster; for the lowest heat input the cooling rate in constant current process is 11.8 °C/s and for the highest heat input it is 16.1 °C/s. For the pulsed current process at the lowest heat input the cooling rate is 11.9 °C/s and for the highest heat input level the cooling rate is 19.2 °C/s.

5.2 Effect of pulsed current on bead profile

It is seen from Table 5 that for the constant current process as well as the pulsed current process, the penetration achieved was less than 50%. For heat input of above 300 J/mm, in constant current process the instance of burn occured. The bead profile was controlled in the pulsed current proess due to the varied heat input to the weld. The width to penetration ratio in the pulsed current process was easily lower than that in the constant current process. For all heat input the values ranged from 2.17 to 5.5 in constant current process. The values for pulsed current process was in from 3.41 to 5.25. The effects of the surface tension and buoyancy forces are seen clearly in all the heat input profiles in constant current and pulsed current processes.

5.3 Effect of pulsed current on tensile properties

The tensile properties were compared for the equal penetration welds. The cooling rates were 14.4 and 12.9 °C/s at 5 mm from weld bead centre, the heat input was 256 J/mm and 232 J/mm, respectively. The yield strength in the constant current process was 185 MPa

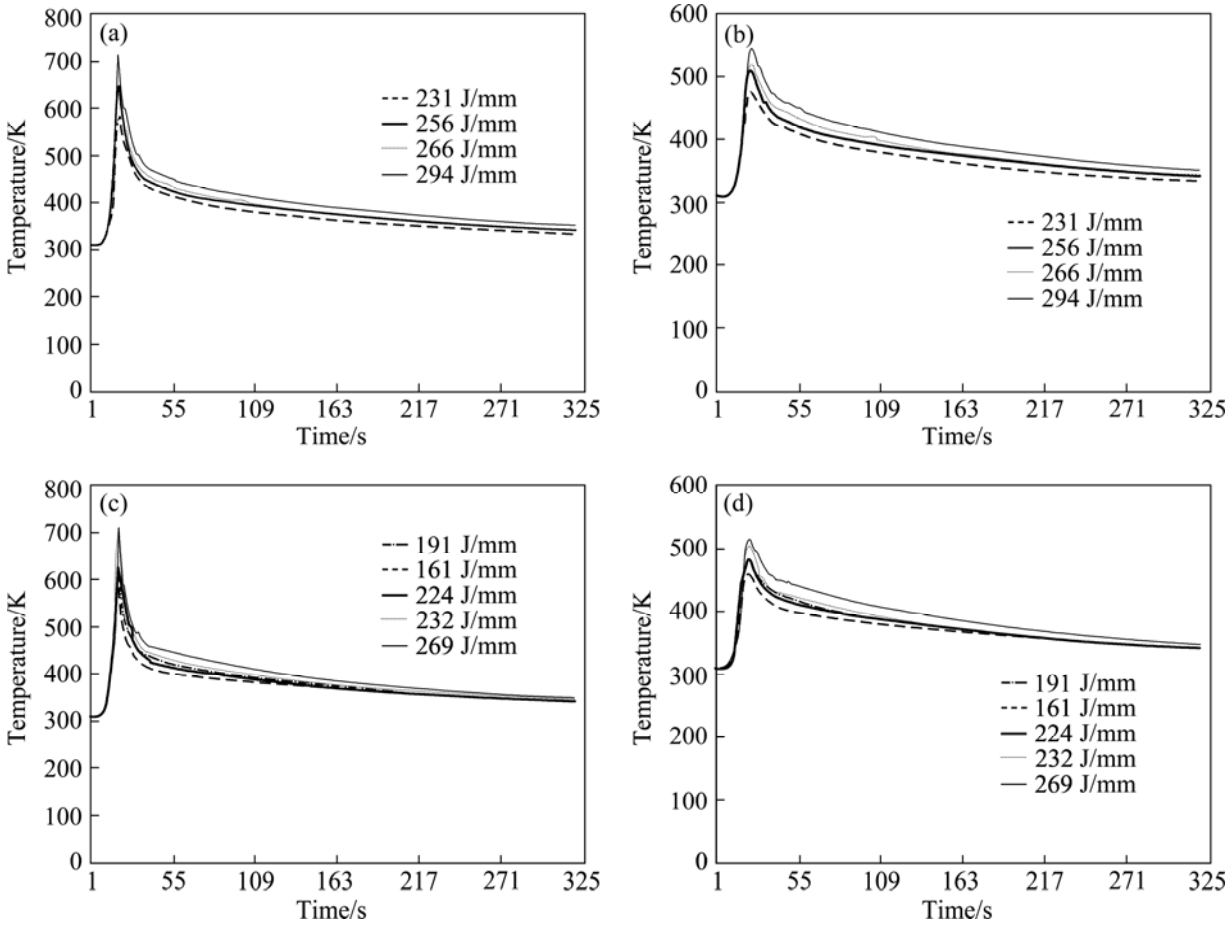

Fig.4 Heating and cooling curves: (a) CC, 5 mm; (b) CC, 15 mm; (c) PC, 5 mm; (d) PC, 15 mm

but in pulsed current process it was 205 MPa and tensile strength followed the same trend as 200 and 225 MPa in the constant current and pulsed current processes respectively. The failure location for both the cases was the weld region. The efficiency of the pulsed current process was 90 % much higher than the joint efficiency of the constant current process. The higher strength is seen in the joint fabricated by the pulsed current.

5.4 Effect of pulsed current on hardness

The micro hardness of the base metal was HV 95. It was evident that in both the cases the hardness was the least at the weld centre and gradually increased at the 5 mm point and further increased at the 15 mm-point. The values of the hardness are less in the constant current joints compared with the pulsed current ones in all the locations. The peak temperatures reached 648 K and 704 K for the constant current and the pulsed current processes respectively at 5 mm-distance from weld centre. The reason for the decrease in the hardness can be attributed to the variation in the temperatures attained and also the pulsing of current in the joint fabricated by the pulsed current. Hence the higher hardness is attributed to the joints fabricated by pulsed current.

5.5 Effect of pulsed current on microstructure

The microstructure of the weld centre reveals coarse grains in the constant current weld while in the pulsed current process the grains are fine, the dendrite spacing in the constant current is wider but the pulsed current process reveals narrower spacing. It is also seen that the area of grain boundary is much less in the constant current process compared with the pulsed current process. The effect of faster cooling rate is seen in the microstructure of the pulsed current specimen with domination of smaller grains. The morphology of the constant current one predominates with the columnar grain structure due to the lower cooling rate (due to higher peak current).

In general, the formation of equiaxed grain structure in CCGTAW weld is known to be difficult because of the remelting of heterogeneous nuclei or growth centers ahead of the solid-liquid interface. This is due to the high temperatures in the liquid, thus making survival nuclei difficult. The evolution of microstructure in weld fusion zone is also influenced in many ways by current pulsing. Principally, the cyclic variations of energy input into the weld pool cause thermal fluctuations, one consequence of which is the periodic interruption in the solidification process. As the pulse peak current decays the solid-liquid

interface advance towards the arc, it increasingly becomes vulnerable to any disturbances in the arc form. As current increases again in the subsequent pulse, growth is arrested and remelting of the growing dendrites can also occur. Current pulsing also results in periodic variations in the arc forces and hence an additional fluid flows, which lowers temperatures in front of the solidifying interface. Furthermore, the temperature fluctuations inherent in pulsed welding lead to a continual change in the weld pool size and shape favoring the growth of new grains. It is also to be noted that effective heat input for unit volume of the weld pool would be considerably less in pulse current welds for the average weld pool temperatures are expected to be low[19]. It is important to note that while dendrite fragmentation has frequently been cited as a possible mechanism, and evidence for the same has not been hitherto established or demonstrated. It has been sometimes suggested that the mechanism of dendrite break-up may not be effective in welding because of the small size of the fusion welds and the fine interdendrite spacing in the weld microstructure. Thus grain refinement observed in the PCGTAW welds is therefore believed to be due to other effects of pulsing on the weld pool shape, fluid flow and temperatures. The continual change in the weld pool shape is particularly important. As the direction of maximum thermal gradient at the solid-liquid interface changes continuously, newer grains successively become favourably oriented. Thus, the individual grains grow faster in small distance allowing for more grains grow, resulting in a fine grained structure[20].

5.6 Effect of pulsed current on residual stress

Two specimens were taken to determine the residual stress, one from the conatant current process and the other from pulsed current process. It is seen from the results that both the specimens show tensile stress at the weld centre, 5 mm and 15 mm. The base metal had compressive stress. The weld centre had higher values of tensile stress and decreased further away from it. The value of stress at the weld centre for the constant current process was 134 MPa while that for pulsed current one was 92 MPa. This trend was seen in points at 5 mm and 15 mm from weld centre. The joints fabricated by the pulsed current showed less magnitude of residual stress compared with that by constant current. The characteristic feature can be attributed to the less peak temperature attained during welding of the pulsed current joints.

6 Conclusions

1) The pulsed current welding technique records lower peak temperatures and lower magnitude of residual stresses compared with constant current welding, which is highly preferable for thin sheet welding.

2) The gas tungsten arc welded aluminium alloy joint fabricated by pulsed current welding technique exhibits superior tensile properties compared with constant current welding technique.

3) The formation of finer grains caused by pulsed current is the main reason for enhanced tensile and hardness properties of the joints.

Acknowledgement

The authors wish to express their sincere thanks to the Department of Manufacturing Engineering, Annamalai University, for the facilities provided in this investigation. The authors also wish to acknowledge Dr G Madhusudhan Reddy, Scientist G, Defence Metallurgical Research Laboratory (DMRL), Hyderabad, for extending the residual stress measurement facility.

References

[1] ELANGOVAN K, BALASUBRAMANIAN V. Influences of tool pin profile and tool shoulder diameter on FSP zone formation in AA6061 aluminium Alloy [J]. Journal of Materials & Design, 2008, 28 (2): 362−373.

[2] KUMAR T S, BALASUBRAMANIAN V, SANAVULLAH M Y. Influences of pulsed current tungsten inert gas welding parameters on tensile properties of AA6061 aluminium alloy [J]. Journal of Materials & Design, 2007, 28(2): 2080−2092.

[3] DAVIES C J, GARLAND J G. Solidification structures and properties of fusion welds [J]. Int Mater Review, 1975, 20: 83−106.

[4] KOU S, LE Y. Nucleation mechanism and grain refining of weld metal [J]. Welding Journal, 1986, 65: 305s−313s.

[5] MADHUSUDHAN R G, GOKHALE A A, PRASAD R K. Optimization of pulse frequency in pulsed current gas tungsten arc welding of aluminium-lithium alloy sheets [J]. Journal of Material Science &Technology, 1998, 14: 61−66.

[6] POTLURI N B, GHOSH P K, GUPTA P C, REDDY Y S. Studies on weld metal characteristics and their influences on tensile and fatigue properties of pulsed current GMA welded Al-Zn-Mg alloy [J]. Welding Research Supplement, 1996, 75: 62s−70s.

[7] MOHANDAS T, MADHUSUDHANA R G. Effect of frequency of pulsing in gas tungsten arc welding on the microstructure and mechanical properties of titanium alloy welds [J]. J Mater Sci Lett, 1996, 15: 626−628.

[8] BALASUBRAMANIAN V, RAVISANKAR V, MADHUSUDHAN REDDY G. Effect of pulsed current and post weld aging treatment on tensile properties of argon arc welded high strength aluminium alloy [J]. Materials Science and Engineering A, 2007, 459: 7−18.

[9] BALASUBRAMANIAN M, JAYABALAN V, BALASUBRAMANIAN V. A mathematical model to predict impact toughness of pulsed current gas tungsten arc welded titanium alloy [J]. International Journal of Advanced Manufacturing Technology, 2008, 35: 852−858.

[10] LU M, KOU S. Power and current distribution in gas tungsten arcs [J]. Weld J, 1988, 67(2): 29s−33s.

[11] SADEK C, ABSI ALFARO K S. CHAWLA & JOHN NORRISH K S. Computer based data acquisition for welding research and production [J]. Journal of Materials Processing Technology, 1995, 53: 1−13.

[12] PETER R N. Childs practical temperature measurements [M]. USA: Elsevier Publications. 1998.
[13] SUNAR M, YILBAS B S, BORAN K. Thermal and stress analysis of a sheet metal in welding [J]. Journal of Materials Processing Technology, 2006, 172: 123−129.
[14] SCOTT P. Selecting a welding frequency [EB/OL]. http://www.thermatool.com/, 2008−06.
[15] GONSALVES C V, VILARINHO L O, SCOTTI A, GUIMARAES G. Estimation of heat source and thermal efficiency in GTAW process by using inverse techniques [J]. Journal of Materials Processing Technology. 2006, 172: 42−51.
[16] KIM W H, NA S J. Heat and fluid flow in pulsed current GTA weld pool [J]. International Journal of Heat and Mass Transfer, 1998, 41: 3213−3227.
[17] FAN H G, SHI Y W, NA S J. Numerical analysis of the arc in pulsed current gas tungsten arc welding using a boundary-fitted coordinate [J]. Journal of Materials Processing Technology, 1997, 72: 437−445.
[18] LOTHONGKUM G, CHAUMBAI P, BHANDHUBANYONG P. TIG pulse welding of 304L austenitic stainless steel in flat, vertical and overhead positions [J]. Journal of Materials Processing Technology, 1999, 89−90: 410−414.
[19] RAVISANKAR V, BALASUBRAMANIAN V. Optimising the pulsed TIG welding parameters to refine the fusion zone [J]. Science and Technology of Welding & Joining, 2006, 11(6): 112−116.
[20] NORMAN A F, HYDE K, COSTELLO F, THOMPSON S, BIRLEY S, PRAGNELL P B. Examination of the effect of Sc on 2000 and 7000 series aluminium castings: for improvements in fusion welding [J]. Materials Science and Engineering A, 2003, A354: 188−198.

脉冲电流对气体保护焊铝合金焊接接头的温度、焊缝和性能的影响

N. KARUNAKARAN[1], V. BALASUBRAMANIAN[2]

1. Department of Mechanical Engineering, Annamalai University, Annamalai Nagar 608002, India;
2. Centre for Materials Joining and Research, Department of Manufacturing Engineering, Annamalai University, Annamalai Nagar 608002, India

摘　要：比较了在恒电流和脉冲电流条件下，气体保护焊铝合金接头的温度分布和焊缝外形，研究了脉冲电流对铝合金接头的拉伸性能、硬度分布、微观组织特征和残余应力分布的影响。与恒电流焊接相比，由于在熔池发生了晶粒细化，使用脉冲电流焊接可以提高焊缝的拉伸性能。

关键词：铝合金；气体保护焊；脉冲电流；温度分布；焊缝；拉伸性能

(Edited by LI Xiang-qun)